Photochemical & Photobiological Sciences

RSC Publishing

PAPER

View Article Online
View Journal

Cite this: DOI: 10.1039/c3pp25362g

Fluorescent photoremovable precursor (acridin-9-ylmethyl)ester: synthesis, photophysical, photochemical and biological applications†

Avijit Jana,[a] Biswajit Saha,[b] S. Karthik,[a] Sharabani Barman,[a] Mohammed Ikbal,[a] Sudip Kumar Ghosh[b] and N. D. Pradeep Singh*[a]

A series of carboxylic acids including amino acids were protected as their corresponding fluorescent ester conjugates by coupling with an environment sensitive fluorophore 9-methylacridine. Photophysical properties of all the ester conjugates along with the protecting group have been investigated. Interestingly, the emission properties of the ester conjugates and 9-methylacridine were found to be highly sensitive to polarity, H-bonding and pH of the environment. Photolysis of all the ester conjugates was carried out using UV light above 360 nm and it was found that in every case the corresponding carboxylic acids were released in high chemical yield. Further, intercalation and the preferred binding mode of acridine-9-methanol and its ester conjugates with DNA were studied. *In vitro* biological studies revealed that acridine-9-methanol has good biocompatibility, cellular uptake property and cell imaging ability.

Received 31st October 2012,
Accepted 13th March 2013

DOI: 10.1039/c3pp25362g

www.rsc.org/pps

1. Introduction

In recent years there has been a growing demand for fluorescent photoremovable protecting groups (PRPGs) especially in the area of drug and gene delivery, due to their unique ability to perform both as "phototrigger" for the drug release and "fluorophore" for cell imaging. To meet the growing need, several fluorescent PRPGs have been synthesized using either of these two strategies: (i) modifying directly fluorophores into fluorescent PRPGs or (ii) covalently attaching an external fluorophore to the existing non-fluorescent PRPGs. Based on the former strategy, fluorophores based on polycyclic aromatic and heteroaromatic compounds such as anthraquinone,[1] pyrene,[2,3] perylene,[4] phenanthrene,[1] anthracene,[5] fluorescein[6] and coumarins[7,8] have been successfully modified as fluorescent PRPGs for various functional groups.

Recently, coumarin[9] based fluorescent PRPGs have been extensively utilized in the construction of a drug delivery system for cancer therapy. Although coumarin based fluorescent PRPGs showed precise control over the anticancer drug release, to a larger extent these fluorescent PRPGs were found to have no specific type of interaction with the DNA and hence they are mostly localized in the cytoplasm of the cell. By any means, if we can develop fluorescent photoremovable protecting groups which can bind with DNA, then we can aim to release the anticancer drug precisely in the cell nucleus, so that it damages the DNA to stop proliferation of the cell.

Acridine is a well known pH sensitive dye that exhibits a difference in fluorescence lifetime between the neutral and protonated states, over the 6.0 to 8.0 pH range in solution. The neutral acridine exhibits a lifetime of ~10 ns, while the protonated form has a lifetime of 31 ns.[10] In addition, the pH sensitive acridine dye is also known to bind tightly but reversibly to DNA by intercalation.[11] Hence, acridine derivatives have been utilized as a carrier to target the cell nucleus.[12,13] Mainly, DNA alkylating agents are targeted to DNA by tethering with acridine molecules.[14] Recently acridine derivatives have been utilised as a multi-targeting anticancer drug, because of their dual ability to intercalate with DNA and to inhibit topoisomerase enzymes.[15,16] The above interesting pH sensitive fluorescence behaviour and intercalating ability of the acridine moiety prompted us to develop one of its derivatives as a pH-sensitive fluorescent PRPG with nuclear targeting ability. Initially, Zhuang *et al.*[17] showed that acridin-9-ylmethyl chromophore can act as a PRPG for alcohols. Recently, Piloto *et al.*[18] also demonstrated that 9-methylacridine chromophore can also be successfully used as a PRPG for amino acids. However, the photophysical properties, nuclear targeting ability, cell imaging studies and cytotoxicity of caged compound of 9-methylacridine and its photoproduct have not yet been investigated.

In this paper, we report a novel environment-sensitive fluorescent PRPG 9-methylacridine for carboxylic acids and amino

[a]Department of Chemistry, Indian Institute of Technology Kharagpur, Kharagpur-721302, India. E-mail: ndpradeep@chem.iitkgp.ernet.in
[b]Department of Biotechnology, Indian Institute of Technology Kharagpur, Kharagpur-721302, India

†Electronic supplementary information (ESI) available. See DOI: 10.1039/c3pp25362g

acids. Environment sensitive fluorescence behaviours of 9-methylacridine and its ester conjugates were investigated. The photorelease ability of 9-methylacridine was studied by irradiating the ester conjugates using UV light above 360 nm. Further, we also investigated the intercalation and the preferred binding mode of the 9-methylacridine and its ester conjugates with DNA using molecular docking studies. *In vitro* cellular imaging and cytotoxicity of 9-methylacridine and ester conjugates were explored.

2. Results and discussion

2.1. Synthesis of ester conjugates of 9-methylacridine (4a–k)[18]

First, 9-methylacridine (**1**) was converted to 9-(bromomethyl)-acridine (**2**) by bromination with *N*-bromo succinimide (NBS) in the presence of benzoyl peroxide in carbon tetrachloride (CCl_4) under reflux for 2 h.[19] Next, the treatment of **2** with N-protected amino acids (**3a–e**) and carboxylic acids (**3f–k**) in the presence of potassium carbonate (K_2CO_3) in dry DCM at room temperature resulted in ester conjugates (**4a–k**) with good to excellent yield (82–90%, Table 1) as shown in Scheme 1.

Table 1 Reaction time and synthetic yield for the protection of amino acids and carboxylic acids

Ester	Acid	Time (h)	Yield[a] (%)
4a	$NH(Boc)CH_2CO_2H$	6	90
4b	$NH(Boc)(CH_2)_3CO_2H$	6	82
4c	$CH_3CH(NHBoc)CO_2H$	8	87
4d	$PhCH_2CH(NHBoc)CO_2H$	6	85
4e	$PhCH_2CH(NHCOPh)CO_2H$	7	89
4f	CH_3CO_2H	8	89
4g	2-(Naphthalen-5-yl)acetic acid	8	85
4h	Benzoic acid	9	88
4i	4-Methoxybenzoic acid	6	87
4j	4-Ethoxy-3-methoxybenzoic acid	7	88
4k	4-Chlorobenzoic acid	6	93

[a] Based on isolated yield.

2.2. Photophysical properties of ester conjugates (4a–k)

2.2.1. UV/vis absorption and fluorescence spectra of ester conjugates (4a–k) in absolute ethanol. UV/vis absorption and fluorescence properties of a degassed 1×10^{-4} M solution of ester conjugates (**4a–k**) along with the protecting group 9-methylacridine (**1**) in absolute ethanol were recorded. The absorption and emission maxima, molar absorptivity, and fluorescence quantum yields of all the ester conjugates along with the protecting group **1** are summarized in Table 2. Fluorescence quantum yield was calculated using 9,10-diphenyl anthracene as a standard (Φ = 0.95 in ethanol).[20]

Fig. 1a and b depicts the normalized absorption and emission spectra of the ester conjugate **4i** and **1** respectively in absolute ethanol. The absorption spectrum of both **4i** and **1** showed an intense band at 360 nm with log ε 4.08, while the emission spectrum was found to be red shifted to about 430 nm. The absorption and emission spectra of all the other ester conjugates in absolute ethanol were found to be almost similar to **1** (see ESI, p. 9, Fig. S.1 and S.2† respectively), suggesting that only the acridine moiety dictates the shape as well as the position of the absorption and the emission spectra of the ester conjugates and the counterpart carboxylic and amino acid have minimal influence on the absorption and emission spectra.

2.2.2. Fluorescence properties of the ester conjugate 4i in neat solvents. The fluorescence intensity and lifetime of nitrogen heterocycles are known to be sensitive to solute–solvent and hydrogen-bond interactions.[21] Thus, to check whether the fluorescence properties of our newly synthesized ester conjugates are sensitive to solvent nature, ester conjugate **4i** was

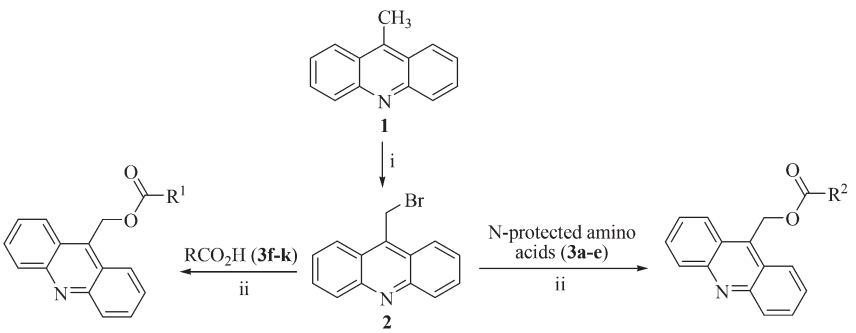

R^1/R^2 = carboxylic acid/amino acid residues

R^1 = (**4f**) Methyl
(**4g**) 1-Naphthyl methyl
(**4h**) Phenyl
(**4i**) 4-Methoxy phenyl
(**4j**) 4-Ethoxy-2-methoxy phenyl
(**4k**) 4-Chloro phenyl

R^2 = (**4a**) CH_2NHBoc
(**4b**) $(CH_2)_3NHBoc$,
(**4c**) $CH(CH_3)NHBoc$,
(**4d**) $CH(CH_2Ph)NHBoc$,
(**4e**) $CH(CH_3)NHCOPh$

Reagents and conditions: (i) NBS, $(PhCO)_2O_2$, CCl_4, reflux, (ii) K_2CO_3, DCM, r.t,

Scheme 1 Synthesis of ester conjugates of 9-methylacridine (**4a–k**).

taken as the model compound and it was excited at 355 nm and the emission spectra were recorded in various solvents.

The fluorescence spectra displayed in Fig. 2 show that the fluorescence properties of the ester conjugate **4i** are strongly influenced by the nature of the solvent. In nonpolar solvents (*e.g.*, *n*-hexane) the ester conjugate **4i** showed weak fluorescence with a maximum emission wavelength of 385 nm, while in a polar solvent (*e.g.* ACN) the emission spectrum becomes structured with slight enhancement in fluorescence intensity along with a red shift. But in an H-bonding donor solvent (*e.g.* MeOH, EtOH) a large red shift of the emission spectrum with strong enhancement of fluorescence intensity was noted. The above fluorescence solvatochromism of the ester conjugate **4i** can be attributed to its closely lying $^1\pi$–π^* and ^{1}n–π^* excited states. Theoretical calculations showed that the ^{1}n–π^* state of acridine is of lower energy than that of the $^1\pi$–π^* state by 0.16 eV.[22] Hence, in nonpolar solvents, non-fluorescent n–π^* transition is the lowest energy transition.[22] But in a hydrogen-bond donor solvent (*e.g.*, methanol, ethanol), due to the hydrogen-bonding interactions between the lone pair electron of the nitrogen atom of acridine and protic solvent, the ^{1}n–π^* excited state energy increases. Thus in a polar protic solvent, we observed inversion in energy level of the excited states and the emissive $^1\pi$–π^* becomes the LUMO resulting in an increased intensity of fluorescence.

2.2.3. Fluorescence properties of the ester conjugate 4i in aqueous binary mixtures. Further, to understand the effect of hydrogen bonding interaction on the fluorescence properties of ester conjugates, we recorded the emission spectra of **4i** in acetonitrile–water mixtures.

We observed that on the addition of increasing amounts of water the fluorescence intensity of the ester conjugate **4i** gradually increases and reaches a maximum in a 60% water–acetonitrile mixture (Fig. 3). Further increase of water content resulted in a large red shift of the fluorescence spectra, which

Table 2 UV/vis absorption and fluorescence data of ester conjugates (**4a–k**) and 9-methylacridine (**1**) in absolute ethanol

	UV/vis absorption		Fluorescence		
Ester	λ_{max} [a] (nm)	log ε [b]	λ_{max} [c] (nm)	Stokes' shift[d] (nm)	Φ_f [e]
4a	360	4.06	435	75	0.033
4b	361	4.07	436	75	0.037
4c	361	4.06	435	74	0.038
4d	360	4.06	436	76	0.036
4e	361	4.07	436	75	0.038
4f	361	4.07	433	72	0.032
4g	360	4.06	432	72	0.033
4h	361	4.07	430	69	0.032
4i	360	4.07	429	69	0.033
4j	361	4.08	427	66	0.036
4k	359	4.08	426	67	0.035
1	361	4.08	433	72	0.040

[a] Maximum absorption wavelength. [b] Molar absorption coefficient at the maximum absorption wavelength. [c] Maximum emission wavelength. [d] Stokes' shift. [e] Fluorescence quantum yield (excitation wavelength 355 nm).

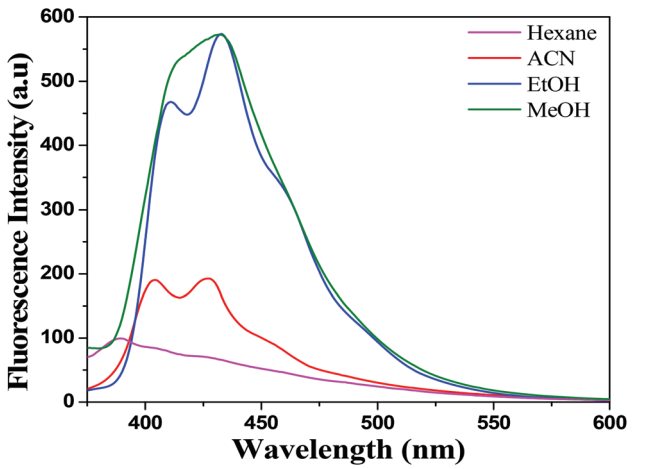

Fig. 2 Corrected fluorescence spectra of the ester conjugate **4i** in different solvent systems.

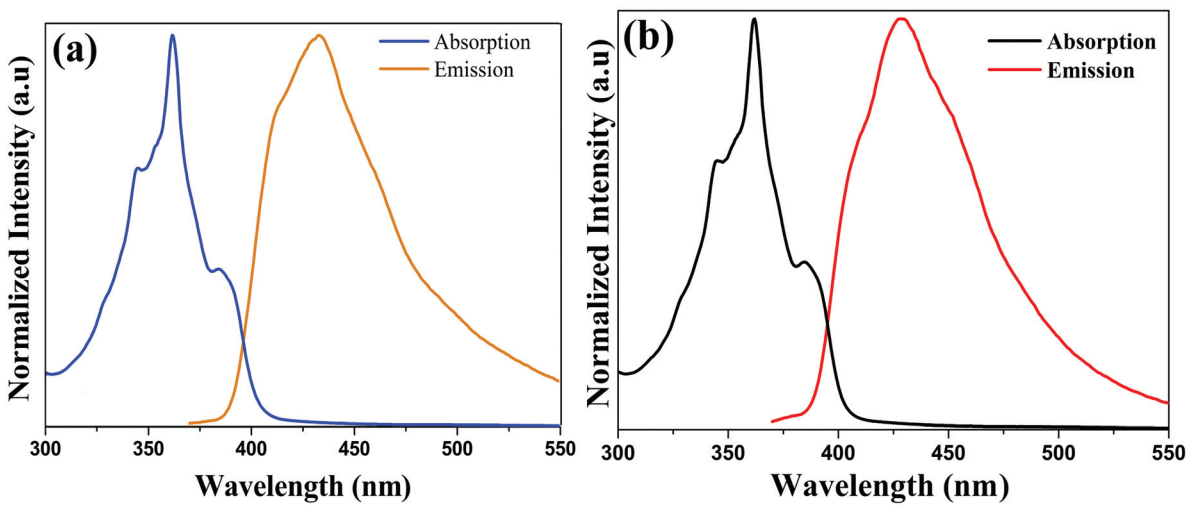

Fig. 1 Normalized absorption and emission spectra of (a) the ester conjugate **4i** and (b) protecting group **1** in ethanol.

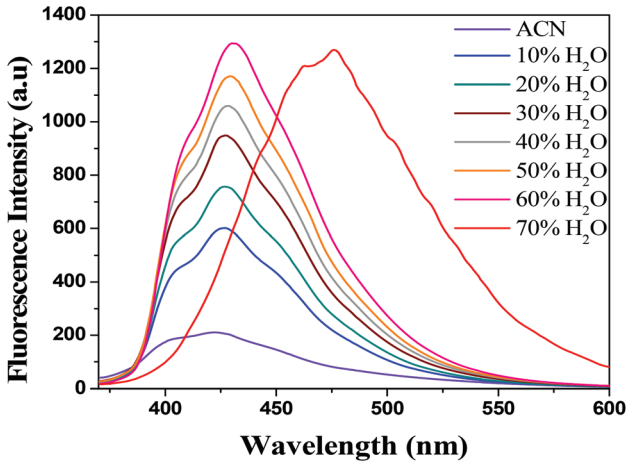

Fig. 3 Corrected fluorescence spectra of the ester conjugate **4i** in an ACN–H_2O mixture (1×10^{-4} M).

may be attributed to the protonation of the acridine "N" atom to produce acridinium cation.[23]

2.2.4. Fluorescence spectra of the ester conjugate 4i at different pH values. To investigate the pH sensitive fluorescence behavior of the ester conjugates, ester conjugate **4i** was taken as the model compound and it was excited at 355 nm and the emission spectra were recorded at different initial pH values. Fig. 4 shows that fluorescence properties of the ester conjugate **4i** are dependent on the pH of the medium. Similar to acridine,[23] we also noted a gradual red shift of the fluorescence spectra of conjugate **4i** as we proceeded towards lower pH (Fig. 4). This is because at lower pH, protonation is favoured and hence protonated **4i** is the predominant species. Thus the fluorescence spectrum at lower pH is mainly observed due to protonated **4i** in the excited state (red line in Fig. 4), whereas at neutral pH, the fluorescence spectrum obtained corresponds to **4i** in the excited state (blue line in Fig. 4). The fluorescence maximum of **4i** in the excited state appears at ≈430 nm, whereas that of protonated **4i** appears at ≈475 nm.

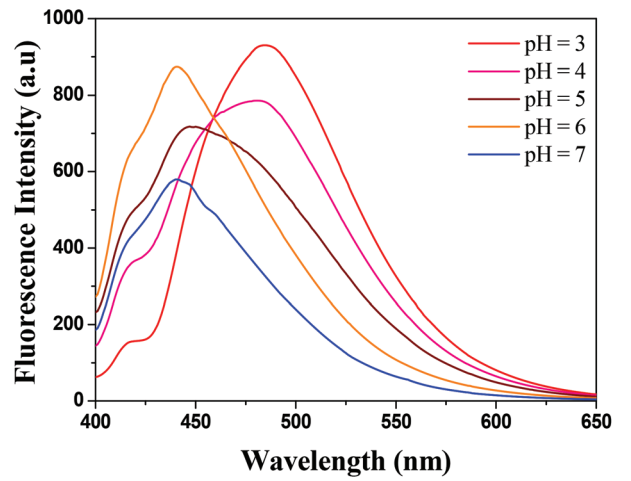

Fig. 4 Steady state fluorescence spectra of the caged ester **4i** (1×10^{-4} M) in water at different pH values.

The photophysical studies showed that **1** and its ester conjugates exhibited strong fluorescence, large Stokes' shift, moderate fluorescence quantum yield, and more interestingly their fluorescence properties are highly sensitive to the solvent polarity, hydrogen bonding ability of the solvent and pH of the medium, which implies that 9-methylacridine chromophore can be targeted as a potential environment sensitive fluorophore.

2.3. Photolysis of ester conjugates (4a–k)

2.3.1. Photolysis of ester conjugates (4a–k) in the acetonitrile–water system. Considering our main interest in studying the application of (acridin-9-ylmethyl)esters as photoremovable precursors for carboxylic and amino acids, we carried out photolysis of caged esters (**4a–k**) (5 mL of 1.0×10^{-4} M solution) individually in acetonitrile–H_2O (50 : 50 v/v) using a 125 W medium pressure Hg lamp as the light source (≥360 nm) and a 10% $CuSO_4$ solution in 0.1 N H_2SO_4 as the UV cut-off filter. We found that all the caged esters released their corresponding carboxylic acids (**4a–k**) (Scheme 2) in high chemical (90–95%) and moderate quantum (0.019–0.025) yields (Φ_p) as summarized in Table 3.

The quantum yield (Φ_p) for the release of carboxylic acids was calculated using potassium ferrioxalate as an actinometer.[24,25] The course of the photocleavage reaction was monitored by reverse phase HPLC.

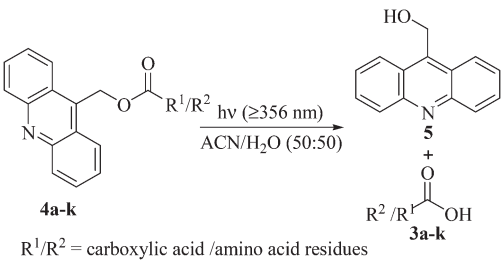

Scheme 2 Photorelease of carboxylic and amino acids.

Table 3 Photolytic data of caged esters (**4a–k**) on UV irradiation (≥360 nm) in an acetonitrile–H_2O (50 : 50) solution

Ester	Irradiation time[a] (min)	% of ester depleted[b]	% of acid released[c]	Quantum yield (Φ_p)[d]
4a	50	97	95	0.020
4b	50	95	92	0.019
4c	50	97	95	0.020
4d	45	93	90	0.022
4e	60	95	92	0.019
4f	50	96	93	0.020
4g	50	95	90	0.021
4h	50	96	92	0.020
4i	45	96	92	0.025
4j	45	96	90	0.025
4k	50	94	90	0.021

[a] Time of UV irradiation. [b] % of ester depleted as determined by HPLC. [c] % of carboxylic acid released as determined by HPLC. [d] Photochemical quantum yields for the release of carboxylic acids (error limit within ±5%).

As a representative example, we have shown in Fig. 5 the HPLC analysis of the reaction mixture of caged ester **4i** at regular intervals of irradiation. The HPLC analysis showed gradual depletion of the peak at t_R 3.84 min with an increase in irradiation time, demonstrating the photo-decomposition of the caged ester **4i**. On the other hand, we also noted a gradual increase of two new major peaks at t_R 3.07 min and t_R 2.40 min, corresponding to the photoproducts acridine-9-methanol (**5**) and 4-methoxybenzoic acid (**3i**) respectively.

In a similar fashion HPLC was used to monitor the photolysis of all other ester conjugates. The normalized peak area obtained from the HPLC analysis in various solvents for the starting ester (**4d–e**, **4i–j**) and the corresponding carboxylic acid (**3d–e**, **3i–j**) released was plotted as a function of irradiation time (Fig. 6a and b). We obtained exponential decay curves for the consumption of the starting ester conjugates, whereas we obtained exponential growth curves for the released acids.

2.3.2. The effect of solvent on the photodecomposition of ester conjugates. To understand the effect of solvent on the photodecomposition of ester conjugates, we carried out photolysis of the conjugate **4i** in different solvents and the results are summarized in Table 4.

We noticed that ester conjugate **4i** released 4-methoxybenzoic acid **3i** more efficiently in the acetonitrile–H_2O (50 : 50) solvent system compared to methanol–H_2O (50 : 50), THF–H_2O (50 : 50) and dioxane–H_2O (50 : 50). HPLC analysis of decomposition of ester **4i** and the formation of carboxylic acid **3i** in various solvents as a function of time is plotted (Fig. 7a and b).

Table 4 Photolytic data of conjugate ester **4i** on irradiation by UV light (≥360 nm) in different solvents

Solvent	Photolytic data of ester conjugate **4i**		
	% of **4i** depleted[a]	% of **3i** released[b]	Quantum yield (Φ_p)[c]
CH_3CN	7	6	0.002
CH_3CN–H_2O (90 : 10)	15	15	0.004
CH_3CN–H_2O (70 : 30)	63	60	0.016
CH_3CN–H_2O (50 : 50)	95	95	0.025
THF–H_2O (50 : 50)	90	84	0.022
CH_3OH	64	60	0.016
CH_3OH–H_2O (50 : 50)	93	90	0.023

[a] % of **4i** depleted as determined by HPLC. [b] % of acid released as determined by HPLC. [c] Photochemical quantum yield for the release of **4i** (error limit within ±5%).

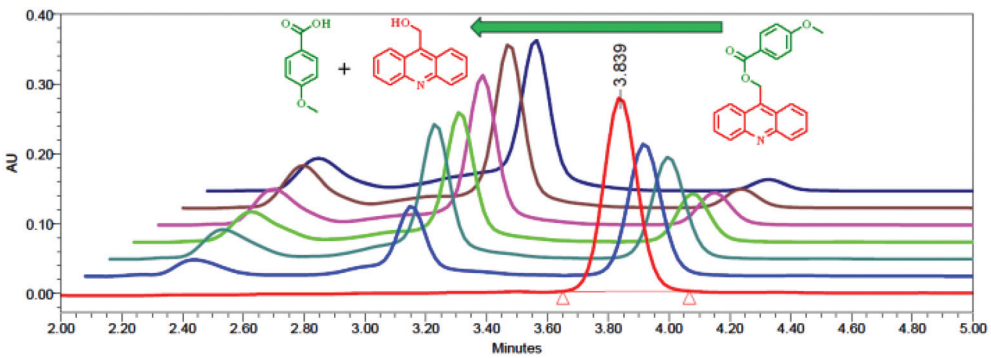

Fig. 5 HPLC analysis of the caged ester (**4i**) at regular intervals of time of photolysis. The *y* axis is offset by 20 mAU and the *x* axis is offset by 5 s for better visualization.

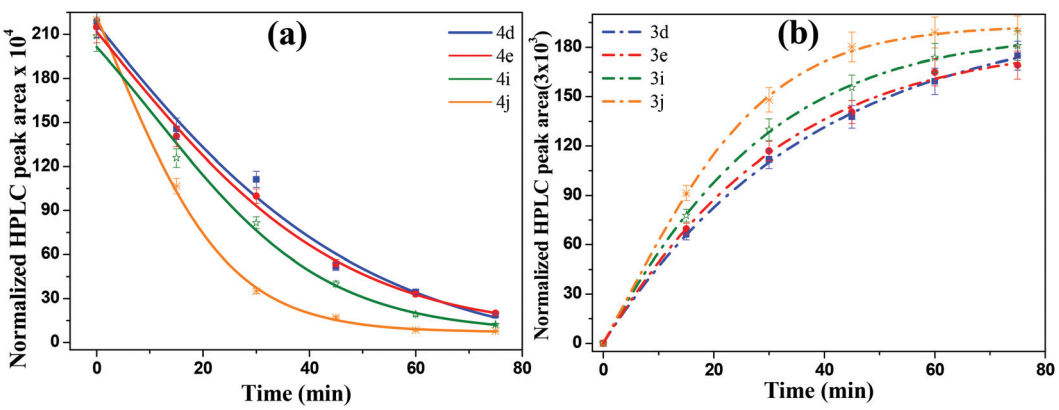

Fig. 6 Normalized HPLC peak area [*A*] *versus* irradiation time for (a) the decomposition of the ester conjugates (**4d–e**, **4i–j**) and (b) the formation of the carboxylic acids (**3d–e**, **3i–j**) in ACN–H_2O (50 : 50) solvent systems. [*A*] was determined by HPLC and is the average of 3 runs (error limit ±5%).

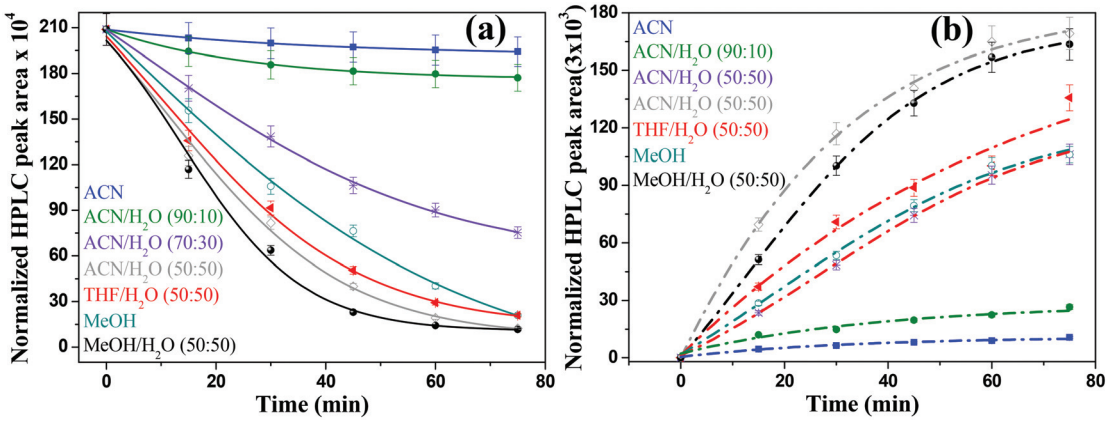

Fig. 7 Normalized HPLC peak area [*A*] *versus* irradiation time for (a) the photolysis of ester conjugate **4i** and (b) the release of the corresponding carboxylic acid **3i** in different solvent systems. [*A*] was determined by HPLC and is the average of 3 runs (error limit ±5%).

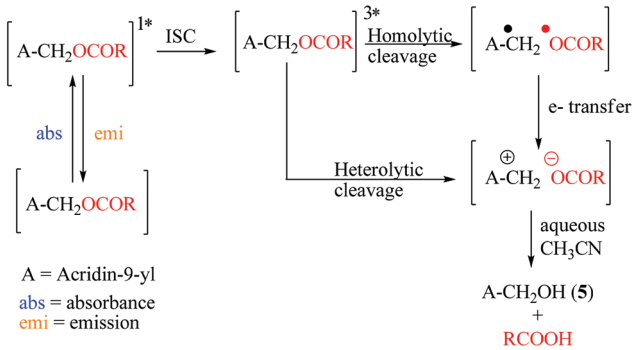

Scheme 3 Possible mechanism for the photorelease of carboxylic and amino acids by 9-methylacridine.

Further, we also noted that as the amount of water in acetonitrile increases, the quantum yield for the photorelease of caged ester **4i** gets increased (quantum yield for the release of 4-methoxybenzoic acid by caged ester **4i** increased by ~4 times as we move from 10% to 30% of water in acetonitrile). The increased quantum yields were attributed to the better stabilization of the newly generated ion pair (Scheme 3) by solvation; a similar phenomenon was also noted in the case of caged anthracene[5] and caged coumarins.[7,8]

2.3.3. Mechanism of the photolysis of ester conjugates. Based on the literature studies reported by Singh *et al.*[5] and Schade *et al.*,[7] we suggest that the photolysis of ester conjugates proceeds through an ionic mechanism. The initial photochemical step involves excitation of the acridin-9-ylmethyl chromophore to its singlet excited state, which then undergoes facile singlet–triplet intersystem crossing. Subsequently, from the triplet excited state it undergoes either homolytic C–O bond cleavage followed by an electron transfer to produce acridin-9-yl methyl carbocation and the carboxylate anion or it may undergo heterolytic C–O bond cleavage to produce the already mentioned ion pair. In an aqueous acetonitrile solvent, the methylenic carbocation and the carboxylate anion react with solvent molecules to yield acridin-9-yl methanol and carboxylic acid respectively (Scheme 3).

2.4. Intercalation and the preferred binding mode of acridine-9-methanol and its ester conjugates

To substantiate the intercalation and the preferred binding mode of the acridine-9-methanol (**5**) and its ester conjugates (**4a–e**) with DNA, we performed molecular docking studies. The docking analysis revealed that the planar ring structure of acridine intercalates between nitrogenous base pairs of the DNA double helix (Fig. 8a–f). Thus the docking study corroborates the experimental findings, which suggests that ester conjugates are behaving as DNA-intercalators.

2.5. *In vitro* cellular imaging studies using ester conjugate (4b) and PRPG acridine-9-methanol (5)

To explore the fluorescence properties of the protecting group (**5**) and the ester conjugate (**4b**), we carried out cellular imaging studies using the L929 cell line obtained from the National Centre for Cell Sciences, Pune (NCCS) which was maintained in Dulbecco's Modified Eagle Medium (DMEM) containing 10% fetal bovine serum at 37 °C and 5% CO_2. Further, we also carried out cellular imaging studies using the HeLa cell line obtained from the National Centre for Cell Sciences, Pune (NCCS). Both cell lines were maintained in minimum essential medium containing 10% fetal bovine serum at 37 °C and 5% CO_2. Cells (5×10^4 cells per well) were plated on 12 well plates and allowed to adhere for 4–8 h. Cells were then incubated with 5×10^{-5} M of compounds **5** and **4b** separately in a cell culture medium for 6 h at 37 °C and 5% CO_2. Thereafter, cells were fixed in paraformaldehyde and washed two times with PBS. Imaging was done in an Olympus confocal microscope (FV1000, Olympus) using a respective filter. Cellular uptake study after 6 h incubation reveals that compounds **5** and **4b** were internalized by the cell membrane and uniformly distributed inside both L929 (Fig. 9) and HeLa cells (Fig. 10).

2.6. Cell cytotoxicity assay of ester conjugate (4b) and photoproduct acridine-9-methanol (5)

The cytotoxicity *in vitro* was measured using the MTT[27] (3-(4,5-dimethylthiazol-2-yl)-2,5-diphenyltetrazolium bromide,

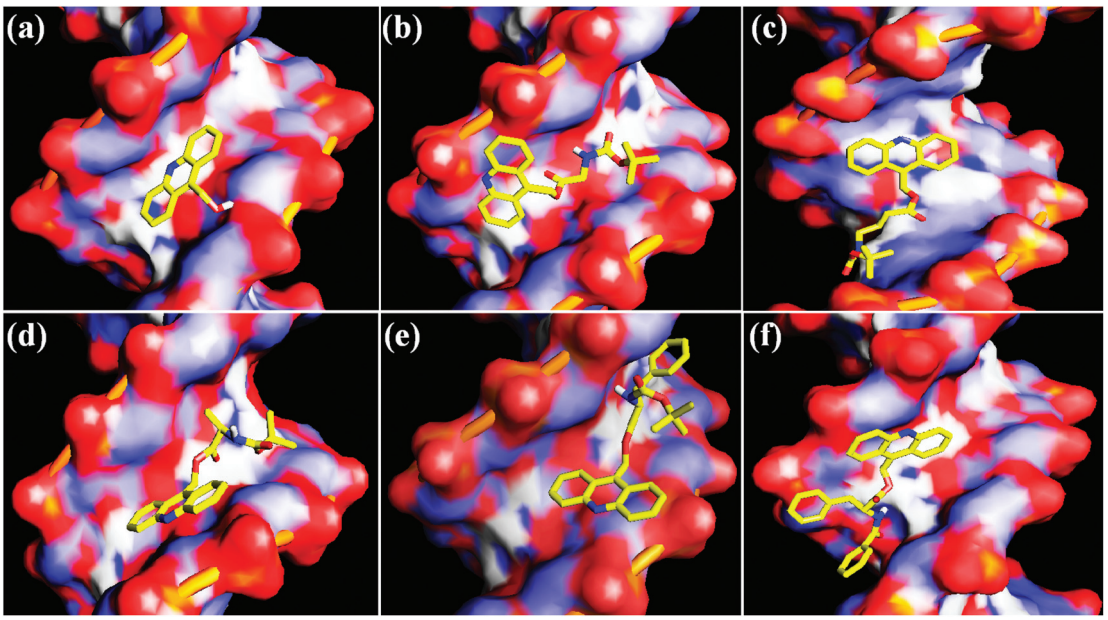

Fig. 8 Surface representation of docked conformations of DNA–acridine caged conjugate complexes showing the binding pockets of conjugate: (a–f) for acridine-9-methanol (**5**) and ester conjugates (**4a–e**) respectively.

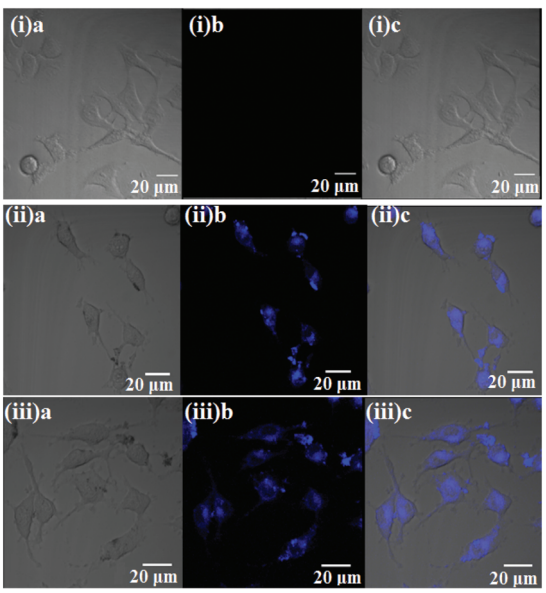

Fig. 9 Confocal fluorescence and brightfield images of L929 cells: (i) untreated cells, (ii) cells incubated with acridine-9-methanol (5×10^{-5} M), (iii) cells incubated with caged ester **4b** (5×10^{-5} M). (a) Brightfield, (b) fluorescence (λ_{ex} 410 nm), and (c) overlay images of (a) and (b). Cells were incubated separately with compounds **5** and **4b** for 6 h.

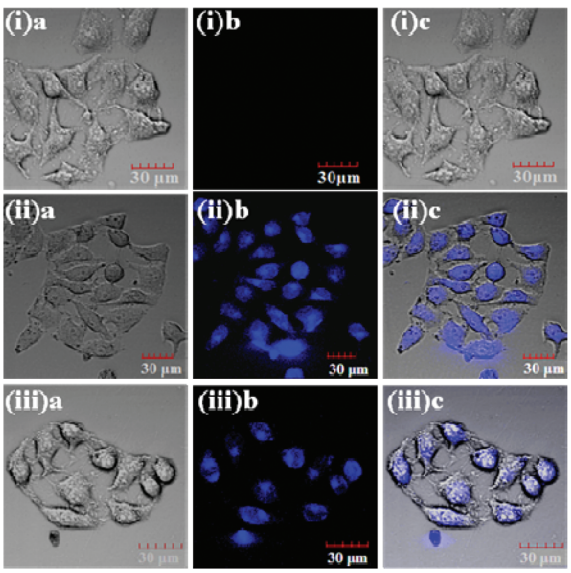

Fig. 10 Confocal fluorescence and brightfield images of HeLa cells: (i) untreated cells, (ii) cells incubated with acridine-9-methanol (5×10^{-5} M), (iii) cells incubated with caged ester **4b** (5×10^{-5} M). (a) Brightfield, (b) fluorescence (λ_{ex} 410 nm), and (c) overlay images of (a) and (b). Cells were incubated separately with compounds **5** and **4b** for 6 h.

a yellow tetrazole) assay in L929 cell line. Briefly, cells growing in the log phase were seeded into a 96-well cell-culture plate at 1×10^4 cells mL^{-1}. Different concentrations of compound **5** and ester **4b** were added in the wells with an equal volume of PBS in the control wells. The cells were then incubated for 72 h at 37 °C in 5% CO_2. Later, fresh media containing 0.40 mg mL^{-1} MTT were added to the above 96-well plates and incubated at 37 °C for an additional 6 h. Thereafter, the medium was removed, the formazan crystals formed were dissolved in DMSO and the absorbance was recorded at 595 nm. The cytotoxic effect of each treatment was expressed as percentage of cell viability relative to the untreated control cells defined as: [[OD 570 nm treated cells]/[OD 570 nm control cells]] × 100.

The percentage of cell viability *vs.* concentration of both compound **5** and caged ester **4b** at different time intervals was

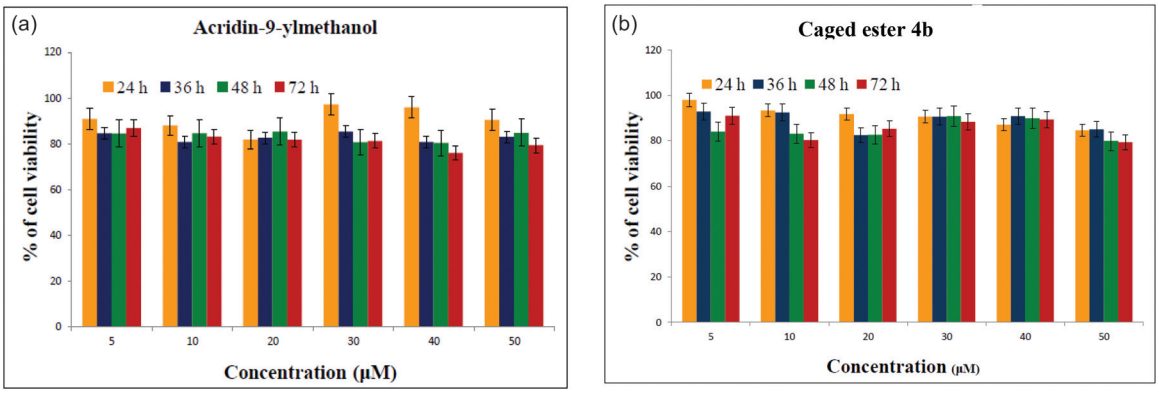

Fig. 11 (a) Cell viability test for **5** against L929 cell line in different concentrations of **5** at different incubation times (values are presented as mean ± standard deviation). (b) Cell viability test for the caged ester **4b** against L929 cell line in different concentrations of **4b** in different incubation times (values are presented as mean ± standard deviation).

presented in Fig. 11a and b respectively, and from the figures it is clear that both compound **5** and caged ester **4b** show insignificant cytotoxicity in any given concentration.

3. Conclusion

In conclusion, we have shown that (acridin-9-ylmethyl)esters can perform dual functions as environment sensitive fluorophores and fluorescent photoremovable precursors for carboxylic and amino acids. Carboxylic acids including amino acids were protected by 9-methylacridine to give their corresponding ester conjugates in good to excellent yield using a simple procedure. Photophysical studies revealed that 9-methylacridine and its ester conjugates showed good fluorescence properties and more interestingly their fluorescence properties were found to be highly sensitive to its surrounding environment. We also demonstrated the ability of (acridin-9-ylmethyl)-esters to release carboxylic acids and amino acids in aqueous organic solvents. Further, we have also shown that acridine-9-methanol and its corresponding ester conjugates can be used for cell imaging studies. Moreover, acridine-9-methanol and its ester conjugates are found to be non-cytotoxic against the L929 cell line up to 50 μM concentration.

4. Experimental section

4.1. General

^{1}H NMR (200 MHz and 400 MHz) spectra were recorded on a BRUKER-AC 200 MHz and a BRUKER-AC 400 MHz spectrometer, respectively. Chemical shifts are reported in parts per million from tetramethylsilane with the solvent resonance as the internal standard (deuterochloroform: 7.26 ppm). Data are reported as follows: chemical shifts, multiplicity (s = singlet, d = doublet, t = triplet, m = multiplet), coupling constant (Hz). ^{13}C NMR (50 MHz) spectra were recorded on a BRUKER-AC 200 MHz spectrometer with complete proton decoupling. Chemical shifts are reported in parts per million from tetramethylsilane with the solvent resonance as the internal standard (deuterochloroform: 77.0 ppm). UV/vis absorption spectra were recorded on a Shimadzu UV-2450 UV/vis spectrophotometer, fluorescence emission spectra were recorded on a Hitachi F-7000 fluorescence spectrophotometer, FTIR spectra were recorded on a PerkinElmer RXI spectrometer and HRMS spectra were recorded on a JEOL-AccuTOF JMS-T100L mass spectrometer. Photolysis of all the ester conjugates was carried out using a 125 W medium pressure mercury lamp supplied by SAIC (India). Chromatographic purification was done with 60–120 mesh silica gel (Merck). For reaction monitoring, precoated silica gel 60 F254 TLC sheets (Merck) were used.

4.2. Synthesis of 9-methylacridine

A mixture of diphenylamine (6.0 g, 36 mmol), acetic acid (6.0 g, 100 mmol) and zinc chloride (25.6 g, 188 mmol) was heated up to 180 °C with continuous stirring. Then excess acetic acid was removed from the reaction mixture by distillation and the reaction mixture was heated at 220 °C for an additional 5 h followed by the addition of an aqueous ammonia solution. The resulting yellow precipitates were collected by filtration. The residue was dissolved in chloroform and neutralized by washing with aqueous $NaHCO_3$ and dried over anhydrous Na_2SO_4. The organic solvent was then removed under reduced pressure to give 5.96 g (87%) of crude product which was further purified by column chromatography using ethyl acetate in pet ether as an eluent.

4.2.1. 9-Methylacridine (5).[26] Yellow solid, mp: 115–120 °C; ^{1}H NMR ($CDCl_3$, 200 MHz): δ = 8.14–8.09 (d, J = 8.8 Hz, 2H), 8.09–8.05 (d, J = 8.8 Hz, 2H), 7.69–7.61 (m, 3H), 7.46–7.38 (m, 3H), 2.93 (s, 3H); ^{13}C NMR ($CDCl_3$, 50 MHz): δ = 148.3 (2C), 142.2 (1C), 130.0 (2C), 129.7 (2C), 125.4 (2C), 125.3 (2C), 124.5 (2C), 13.5 (1C).

4.3. General procedure for the synthesis of ester conjugates (4a–e)

9-(Bromomethyl)acridine (1 equiv.) was dissolved in dry dichloromethane (DCM) (2 mL), potassium carbonate (1.2

equiv.) and the corresponding N-protected amino acid (1 equiv.) were added. The reaction mixture was stirred at room temperature for 6–9 h. The solvent was removed by rotary evaporation under reduced pressure and the crude residue was purified by column chromatography using ethyl-acetate (EtOAc) in pet ether.

The compounds **4a**, **4b** and **4c** were characterized by ^{1}H, ^{13}C NMR, IR and mass spectral analysis and the data matched the literature values.[18]

4.3.1. (*S*)-Acridin-9-ylmethyl 2-(*tert*-butoxycarbonylamino)-3-phenylpropanoate (4d). 9-(Bromomethyl)acridine (0.100 g, 0.37 mmol), potassium carbonate (0.061 g, 0.44 mmol) and *N*-(*tert*-butoxycarbonyl)-L-phenylalanine (0.098 g, 0.37 mmol) were used. The reaction mixture was stirred for 6 h. A yellow residue was obtained which on purification using 25% EtOAc in pet ether gave compound **4d** (0.143 g, 85%) as a yellow solid; mp: 145–148 °C; ^{1}H NMR ($CDCl_3$, 200 MHz): δ = 8.34–8.28 (m, 4H), 7.89–7.81 (m, 2H), 7.69–7.61 (m, 2H), 7.09–6.94 (m, 3H), 6.88–6.85 (d, J = 7.2 Hz, 1H), 6.34–6.27 (d, J = 12.6, 1H), 6.09–6.02 (d, J = 12.6 Hz, 1H), 5.00–4.97 (d, J = 6.8 Hz, 1H), 4.69–4.62 (m, 1H), 3.00–2.97 (d, J = 6.0 Hz, 2H), 1.41 (s, 9H); ^{13}C NMR ($CDCl_3$, 50 MHz): δ = 171.8 (1C), 155.3 (1C), 148.8 (2C), 136.2 (1C), 130.4 (2C), 130.0 (2C), 129.1 (2C), 128.3 (2C), 126.8 (2C), 126.0 (1C), 125.4 (2C), 124.0 (2C), 123.5 (1C), 79.8 (1C), 58.2 (1C), 54.5 (1C), 38.2 (1C), 28.3 (3C); UV/vis (EtOH): λ (log ε) 361 (4.06); HRMS calc. for $C_{28}H_{28}N_2NaO_4$ [M + Na^+]: 479.1947, found: 479.1950.

4.3.2. (*S*)-Acridin-9-ylmethyl 2-benzamido-3-phenylpropanoate (4e). 9-(Bromomethyl)acridine (0.100 g, 0.37 mmol), potassium carbonate (0.061 g, 0.44 mmol) and (*S*)-2-(benzamido)-3-phenylpropanoic acid (0.099 g, 0.37 mmol) were used. The reaction mixture was stirred for 7 h. A brown residue was obtained which on purification using 25% EtOAc in pet ether gave compound **4e** (0.151 g, 89%) as a yellow solid, mp: 120–122 °C; ^{1}H NMR ($CDCl_3$, 200 MHz): δ = 8.34–8.28 (dd, J = 3.2, 8.8 Hz, 4H), 7.87–7.79 (m, 3H), 7.72–7.58 (m, 4H), 7.55–7.48 (m, 4H), 6.97–6.93 (d, J = 8.8 Hz, 3H), 6.35–6.29 (d, J = 12.2 Hz, 2H), 6.11–6.05 (d, J = 12.2 Hz, 1H), 5.18–5.07 (m, 1H), 3.15–3.11 (dd, J = 2.2, 5.8 Hz, 2H); ^{13}C NMR ($CDCl_3$, 50 MHz): δ = 171.5 (1C), 166.9 (1C), 148.7 (2C), 136.2 (1C), 135.3 (1C), 133.7 (1C), 131.9 (1C), 130.2 (2C), 130.1 (2C), 129.1 (2C), 128.6 (2C), 128.4 (2C), 127.1 (2C), 127.0 (1C), 126.9 (2C), 125.3 (2C), 123.9 (2C), 58.4 (1C), 53.7 (1C), 37.8 (1C); FTIR (KBr, cm^{-1}): 3447, 1722, 1631; UV/vis (EtOH): λ (log ε) 361 (4.07); HRMS calc. for $C_{30}H_{24}N_2NaO_3$ [M + Na^+]: 483.1685, found: 483.1689.

4.4. General procedure for the synthesis of caged esters (4f–k)

For the preparation of ester conjugates (**4f–k**) we followed the same procedure as in the case of synthesis of ester conjugates (**4a–e**) except that carboxylic acids were used instead of amino acids.

4.4.1. (Acridin-9-yl)methyl acetate (4f). 9-(Bromomethyl)-acridine (0.100 g, 0.37 mmol), potassium carbonate (0.061 g, 0.44 mmol) and acetic acid (0.022 g, 0.37 mmol) were used. The reaction mixture was stirred for 8 h. A brown residue was obtained which on purification using 20% EtOAc in pet ether gave compound **4f** (0.083 g, 89%) as a yellow solid, mp: 152–155 °C; ^{1}H NMR ($CDCl_3$, 200 MHz): δ = 8.37–8.32 (d, J = 8.8 Hz, 2H), 8.31–8.26 (d, J = 8.8 Hz, 2H), 7.86–7.77 (m, 2H), 7.68–7.59 (m, 2H), 6.12 (s, 2H), 2.11 (s, 3H); ^{13}C NMR ($CDCl_3$, 50 MHz): δ = 170.8 (1C), 148.8 (2C), 136.9 (1C), 130.4 (2C), 129.9 (2C), 126.7 (2C), 125.4 (2C), 124.0 (2C), 57.5 (1C), 20.8 (1C); FTIR (KBr, cm^{-1}): 1733; UV/vis (EtOH): λ (log ε) 360 (4.07); HRMS calc. for $C_{16}H_{13}NNaO_2$ [M + Na^+]: 274.0844, found: 274.0840.

4.4.2. (Acridin-9-yl)methyl 2-(naphthalene-1-yl)acetate (4g). 9-(Bromomethyl)acridine (0.100 g, 0.37 mmol), potassium carbonate (0.061 g, 0.44 mmol) and 2-(naphthalen-1-yl)acetic acid (0.067 g, 0.37 mmol) were used. The reaction mixture was stirred for 8 h. A brown residue was obtained which on purification using 20% EtOAc in pet ether gave compound **4g** (0.118 g, 85%) as a yellow solid, mp: 125–128 °C; ^{1}H NMR ($CDCl_3$, 200 MHz): δ = 8.28–8.18 (4H), 7.85–7.74 (m, 5H), 7.54–7.41 (m, 3H), 7.35–7.27 (m, 3H), 6.12 (s, 2H), 4.08 (s, 2H); ^{13}C NMR ($CDCl_3$, 50 MHz): δ = 171.4 (1C), 148.8 (2C), 136.7 (1C), 133.8 (1C), 131.9 (1C), 130.3 (2C), 129.9 (2C), 128.7 (1C), 128.2 (1C), 128.1 (1C), 126.6 (1C), 126.3 (1C), 125.8 (2C), 125.4 (2C), 125.3 (1C), 124.0 (2C), 123.6 (1C), 58.2 (1C), 39.1 (1C); FTIR (KBr, cm^{-1}): 1735; UV/vis (EtOH): λ (log ε) 361 (4.06); HRMS calc. for $C_{26}H_{20}NO_2$ [M + H^+]: 378.1494, found: 378.1500.

4.4.3. (Acridin-9-yl)methyl benzoate (4h). 9-(Bromomethyl)-acridine (0.100 g, 0.37 mmol), potassium carbonate (0.061 g, 0.44 mmol) and benzoic acid (0.045 g, 0.37 mmol) were used. The reaction mixture was stirred for 9 h. A brown residue was obtained which on purification using 20% EtOAc in pet ether gave compound **4h** (0.102 g, 88%) as a yellow solid, mp: 118–122 °C; ^{1}H NMR ($CDCl_3$, 200 MHz): δ = 8.48–8.44 (d, J = 9.0 Hz, 2H), 8.31–8.27 (d, J = 8.8 Hz, 2H), 8.01–7.98 (d, J = 7.4 Hz, 2H), 7.87–7.78 (m, 2H), 7.69–7.61 (m, 2H), 7.53–7.49 (d, J = 7.4 Hz, 1H), 7.41–7.34 (t, J = 6.8 Hz, 2H), 6.37 (s, 2H); ^{13}C NMR ($CDCl_3$, 50 MHz): δ = 171.4 (1C), 148.5 (2C), 133.6 (1C), 133.4 (1C), 130.3 (3C), 130.2 (1C), 129.8 (2C), 128.9 (2C), 128.5 (2C), 126.9 (1C), 125.6 (2C), 124.1 (2C), 58.1 (1C); FTIR (KBr, cm^{-1}): 1710; UV/vis (EtOH): λ (log ε) 360 (4.07); HRMS calc. for $C_{21}H_{16}NO_2$ [M + H^+]: 314.1181, found: 314.1180.

4.4.4. (Acridin-9-yl)methyl 4-methoxybenzoate (4i). 9-(Bromomethyl)acridine (0.100 g, 0.37 mmol), potassium carbonate (0.061 g, 0.44 mmol) and 4-methoxybenzoic acid (0.056 g, 0.37 mmol) were used. The reaction mixture was stirred for 6 h. A brown residue was obtained which on purification using 20% EtOAc in pet ether gave compound **4i** (0.110 g, 87%) as a yellow solid, mp: 148–150 °C; ^{1}H NMR ($CDCl_3$, 200 MHz): δ = 8.49–8.46 (d, J = 8.8 Hz, 2H), 8.34–8.29 (d, J = 8.6 Hz, 2H), 8.00–7.93 (d, J = 9.0 Hz, 2H), 7.88–7.80 (m, 2H), 7.71–7.63 (m, 2H), 6.90–6.85 (d, J = 9.0 Hz, 2H), 6.36 (s, 2H), 3.84 (s, 3H); ^{13}C NMR ($CDCl_3$, 50 MHz): δ = 166.3 (1C), 163.9 (1C), 149.1 (2C), 137.5 (1C), 132.1 (2C), 130.6 (2C), 130.1 (2C), 126.9 (2C), 125.7 (2C), 124.4 (2C), 122.1 (1C), 113.9 (2C), 58.0 (1C), 55.6 (1C); FTIR (KBr, cm^{-1}): 1710; UV/vis (EtOH): λ (log ε) 360 (4.07);

HRMS calc. for $C_{22}H_{18}NO_3$ [M + H^+]: 344.1287, found: 344.1279.

4.4.5. (Acridin-9-yl)methyl 4-ethoxy-2-methoxybenzoate (4j). 9-(Bromomethyl)acridine (0.100 g, 0.37 mmol), potassium carbonate (0.061 g, 0.44 mmol) and 4-ethoxy-2-methoxybenzoic acid (0.072 g, 0.37 mmol) were used. The reaction mixture was stirred for 7 h. A brown residue was obtained which on purification using 20% EtOAc in pet ether gave compound **4j** (0.126 g, 88%) as a yellow solid; mp: 135–138 °C; ^{1}H NMR ($CDCl_3$, 200 MHz): δ = 8.49–8.45 (d, J = 8.6 Hz, 2H), 8.33–8.29 (d, J = 8.6 Hz, 2H), 7.88–7.79 (m, 2H), 7.70–7.62 (m, 2H), 7.58–7.52 (m, 2H), 6.82–6.78 (d, J = 8.4 Hz, 1H), 6.35 (s, 2H), 4.17–4.07 (q, J = 7.0 Hz, 2H), 3.86 (s, 3H), 1.51–1.44 (t, J = 7.0 Hz, 3H); ^{13}C NMR ($CDCl_3$, 50 MHz): δ = 166.2 (1C), 152.8 (1C), 148.9 (2C), 137.3 (1C), 130.4 (2C), 129.9 (3C), 126.7 (2C), 125.5 (1C), 124.2 (2C), 123.9 (2C), 121.7 (1C), 112.4 (1C), 111.3 (1C), 64.4 (1C), 57.9 (1C), 56.0 (1C), 14.6 (1C); FTIR (KBr, cm^{-1}): 1712; UV/vis (EtOH): λ (log ε) 361 (4.08); HRMS calc. for $C_{24}H_{22}NO_4$ [M + H^+]: 388.1549, found 388.1550.

4.4.6. (Acridin-9-yl)methyl 4-chlorobenzoate (4k). 9-(Bromomethyl)acridine (0.100 g, 0.37 mmol), potassium carbonate (0.061 g, 0.44 mmol) and 4-chlorobenzoic acid (0.058 g, 0.37 mmol) were used. The reaction mixture was stirred for 6 h. A yellow residue was obtained which on purification using 20% EtOAc in pet ether gave compound **4k** (0.119 g, 93%) as a yellow solid, mp: 175–178 °C; ^{1}H NMR ($CDCl_3$, 200 MHz): δ = 8.46–8.41 (d, J = 8.8 Hz, 2H), 8.34–8.29 (d, J = 8.6 Hz, 2H), 7.95–7.91 (d, J = 8.4 Hz, 2H), 7.88–7.83 (m, 2H), 7.71–7.62 (m, 2H), 7.38–7.34 (d, J = 8.4 Hz, 2H), 6.37 (s, 2H); ^{13}C NMR ($CDCl_3$, 50 MHz): δ = 165.5 (1C), 147.9 (2C), 139.9 (1C), 136.6 (1C), 131.2 (2C), 130.5 (2C), 129.9 (2C), 128.8 (2C), 127.9 (1C), 126.9 (2C), 125.5 (2C), 123.9 (2C), 58.3 (1C); FTIR (KBr, cm^{-1}): 1718; UV/vis (EtOH): λ (log ε) 359 (4.08); HRMS calc. for $C_{21}H_{14}ClNNaO_2$ [M + Na^+]: 370.0611, found: 370.0611.

4.5. Photophysical properties of ester conjugates (4a–k)

The UV/vis absorption spectra of degassed 2×10^{-4} M solution of the caged esters (**4a–k**) absolute ethanol were recorded on a Shimadzu UV-2450 UV/vis spectrophotometer, and the fluorescence emission spectra were recorded on a Hitachi F-7000 fluorescence spectrophotometer. Fluorescence quantum yield of ester conjugates was calculated using eqn (1):

$$(\Phi_f)_{CG} = (\Phi_f)_{ST} \frac{(Grad_{CG})}{(Grad_{ST})} \frac{(\eta_{CG}{}^2)}{(\eta_{ST}{}^2)}, \quad (1)$$

where the subscripts CG and ST denote caged compound and standard respectively. 9,10-Diphenyl anthracene in ethanol was taken as a standard. Φ_f is fluorescence quantum yield; Grad is the gradient from the plot of integrated fluorescence intensity *vs*. absorbance, and η is the refractive index of the solvent.

Since, fluorescence for both caged compounds and standard were recorded in the same solvent eqn (1a) was used for the calculation of fluorescence quantum yield.

$$(\Phi_f)_{CG} = (\Phi_f)_{ST} \frac{(Grad_{CG})}{(Grad_{ST})} \quad (1a)$$

4.6. Correction of fluorescence spectra

4.6.1. Excitation spectral correction. Measurement of excitation spectral correction factors was performed using a Rhodamine B quantum counter (3 g L^{-1} in ethylene glycol) and the data were stored automatically by the instrument. Corrected excitation spectra were obtained by using the following equation:

$$I_{FL}(\text{corrected}) = \frac{I_{FL}(\text{uncorrected})}{I_{FL}(\text{quantum counter})}$$

where I_{FL}(corrected) = corrected fluorescence intensity, I_{FL}(uncorrected) = uncorrected fluorescence intensity, I_{FL}(quantum counter) = fluorescence intensity of the quantum counter.

4.6.2. Emission spectral correction. The correction factor for emission spectra was then obtained using the corrected excitation monochromator. The following equation was used to calculate the emission correction factors

$$\text{Emission side correction factor} = \frac{\text{Product of correction factors on EX and EM sides}}{\text{Excitation side correction factor}}.$$

The emission corrections were stored in the computer for performing automatic correction *via* software.

4.7. Deprotection photolysis of ester conjugates (4a–k)

A solution of 10^{-4} M of the caged esters (**4a–k**) was prepared in acetonitrile–H_2O (50 : 50) individually. Half of the solution was kept in the dark and into the remaining half nitrogen gas was passed and irradiated using a 125 W medium pressure Hg lamp as the light source (≥356 nm) and a 1 M $CuSO_4$ in 0.1 N H_2SO_4 solution as a UV cut-off filter. At regular intervals of time, 20 μL of the aliquots was taken and analyzed by RP-HPLC using methanol mobile phase, at a flow rate of 1 mL min^{-1} (detection: UV 254 nm). Peak areas were determined by RP-HPLC, which indicated a gradual decrease of the caged compound with time, and the average of three runs. The reaction was followed until the consumption of the caged compound is less than 5% of the initial area. Further, the quantum yield for the photolysis of caged compounds was calculated using eqn (2)

$$(\Phi_p)_{CG} = \frac{(k_p)_{CG}}{I_0(F_{CG})}, \quad (2)$$

where the subscript 'CG' denotes caged compound. Φ_p is the photolysis quantum yield, k_p is the photolysis rate constant, I_0 is the incident photon flux and F is the fraction of light absorbed. Potassium ferrioxalate was used as an actinometer.

4.8. Preparative photolysis

A solution of ester conjugates (**4a–k**) (0.05 mmol) in acetonitrile–H_2O (50 : 50) individually was irradiated using the

procedure described under section 4.7. The irradiation was monitored by TLC at regular intervals. After completion of photolysis, the solvent was removed under vacuum and the photoproducts acridin-9-ylmethanol and the corresponding carboxylic acid were isolated by column chromatography using increasing percentage of EtOAc in hexane as an eluent.

4.8.1. (Acridin-9-yl)methanol (5).[17,18] Yellow solid, mp: 135 °C; ^{1}H NMR (d^6-DMSO, 200 MHz): δ = 8.57–8.53 (d, J = 8.8 Hz, 2H), 8.21–8.16 (d, J = 8.6 Hz, 2H), 7.91–7.83 (t, J = 7.6 Hz, 2H), 7.72–7.64 (d, J = 7.0 Hz, 2H), 5.66 (bs, 1H, OH), 5.51 (s, 2H); ^{13}C NMR (d^6-DMSO, 50 MHz): δ = 148.3 (2C), 142.3 (1C), 129.9 (2C), 129.6 (2C), 125.8 (2C), 125.3 (2C), 124.4 (2C), 54.7 (1C).

4.9. Hydrolytic stability of caged esters (4a–k) in different solvent pH values

A solution of 10^{-4} M of caged esters (**4a–k**) was prepared in acetonitrile–H_2O (75 : 25), at three different initial pH values (4.5, 6, and 7.5) and kept in the dark for a period of 30 days individually. The course of the hydrolysis reaction was followed by reverse phase HPLC and the percentage of hydrolysis of the corresponding ester conjugate obtained from the HPLC peak area was the average of three runs.

4.10. Acridine-9-methanol and the caged ester 4b for cell imaging studies using L929 cell line

Cell imaging studies were carried out using the L929 cell line obtained from the National Centre for Cell Science (NCCS) which was maintained in minimum essential medium (MEM) containing 10% fetal bovine serum (FBS) at 37 °C and 5% CO_2. To study the cellular uptake of acridine-9-methanol and the caged ester **4b**, briefly L929 cells (5×10^4 cells per well) were plated on 12 well plates and allowed to adhere for 4–8 hours. Cells were then incubated with 5×10^{-5} M of both the compounds separately in the cell culture medium for 6 h at 37 °C and 5% CO_2. Thereafter, cells were fixed in paraformaldehyde for 15 min and washed two times with PBS. Imaging was done in an Olympus confocal microscope (FV1000, Olympus) using the respective filter.

4.11. Acridine-9-methanol and the caged ester 4b for cell imaging studies using HeLa cell line

To check the cellular uptake properties of acridine-9-methanol and the caged ester **4b** on HeLa cell line, we followed the same procedure as described in section 4.10.

4.12. Cytotoxicity of acridine-9-methanol and the caged ester 4b on L929 cell line

The cytotoxicity *in vitro* was measured using the MTT[27] (3-(4,5-dimethylthiazol-2-yl)-2,5-diphenyltetrazolium bromide, a yellow tetrazole) assay on L929 cell line. Briefly, cells growing in the log phase were seeded into a 96-well cell-culture plate at 1×10^4 cells mL^{-1}. Different concentrations of acridine-9-methanol and the caged ester **4b** were added to the wells with an equal volume of PBS in the control wells. The cells were then incubated for 72 h at 37 °C in 5% CO_2. Thereafter, fresh media containing 0.40 mg mL^{-1} MTT were added to the 95 well plates and incubated for 4 h at 37 °C in 5% CO_2. Formazan crystals thus formed were dissolved in DMSO after decanting the earlier media and absorbance was recorded at 595 nm.

4.13. Molecular docking study

Molecular docking studies have been carried to substantiate the interaction and the preferred binding mode of acridine-amino acids caged conjugate with DNA. The crystal structure of DNA was obtained from the Protein Data Bank[28] (PDB entry 3MKY) and was used for the docking studies. The DNA file was prepared for docking by removing water molecules and adding hydrogen atoms with Gasteiger charges. The 3D structure of the ligands was generated in the PRODRG server[29] and its energy-minimized conformation was obtained using accelrys discovery studio 3.1 by applying CHARMM[30] force field with Momany–Rone partial charges. The rotatable bonds in the ligand were assigned with AutoDock Tools and flexible docking was carried out with AutoDock 4.2 Lamarckian Genetic Algorithm (GA).[31] The whole DNA was enclosed in a grid having 0.503 Å spacing for blind-docking purposes. Other miscellaneous parameters were assigned the default values given by AutoDock. The output from AutoDock was rendered in PyMol.[32]

References

1 T. Furuta, Y. Hirayama and M. Iwamura, Anthraquinon-2-ylmethoxycarbonyl (Aqmoc): a new photochemically removable protecting group for alcohols, *Org. Lett.*, 2001, **3**, 1809.
2 M. Iwamura, C. Hodota and M. Ishibashi, 1-(α-Diazobenzyl)pyrene: a reagent for photolabile and fluorescent protection of carboxyl groups of amino acids and peptides, *Synlett*, 1991, 35.
3 M. Iwamura, T. Ishikawa, Y. Koyama, K. Sakuma and H. Iwamura, 1-Pyrenylmethyl esters, photolabile protecting groups for carboxylic acids, *Tetrahedron Lett.*, 1987, **28**, 679.
4 A. Jana, M. Ikbal and N. D. Pradeep Singh, Perylen-3-ylmethyl: fluorescent photoremovable protecting group (FPRPG) for carboxylic acids and alcohols, *Tetrahedron*, 2012, **68**, 1128–1136.
5 A. K. Singh and P. K. Khade, Anthracene-9-methanol-a novel fluorescent phototrigger for biomolecular caging, *Tetrahedron Lett.*, 2005, **46**, 5563–5566.
6 P. Sebej, J. Wintner, P. Müller, T. Slanina, J. A. Anshori, L. A. P. Antony, P. Klán and J. Wirz, Fluorescein analogues as photoremovable protecting groups absorbing at ~520 nm, *J. Org. Chem.*, 2013, **78**, 1833–1843.
7 B. Schade, V. Hagen, R. Schmidt, R. Herbrich, E. Krause, T. Eckardt and J. Bendig, Deactivation behavior and excited-state properties of (coumarin-4-yl)methyl derivatives. 1. Photocleavage of (7-methoxycoumarin-4-yl)methyl-caged acids with fluorescence enhancement, *J. Org. Chem.*, 1999, **64**, 9109–9117.

8 V. Hagen, S. Frings, J. Bendig, D. Lorenz, B. Wiesner and U. B. Kaupp, Fluorescence spectroscopic quantification of the release of cyclic nucleotides from photocleavable [bis-(carboxymethoxy)coumarin-4-yl]methyl esters inside cells, *Angew. Chem., Int. Ed.*, 2002, **41**, 3625–3628.

9 (*a*) Q. Lin, Q. Huang, C. Li, C. Bao, Z. Liu, F. Li and L. Zhu, Anticancer drug release from a mesoporous silica based nanophotocage regulated by either a one- or two-photon process, *J. Am. Chem. Soc.*, 2010, **132**, 10645–10647; (*b*) H.-M. Lin, W.-K. Wang, P.-A. Hsiung and S.-G. Shyu, Light-sensitive intelligent drug delivery systems of coumarin-modified mesoporous bioactive glass, *Acta Biomater.*, 2010, **6**, 3256–3263.

10 A. G. Ryder, S. Power, T. J. Glynn and J. J. Morrison, Time-domain measurement of fluorescence lifetime variation with pH, *Proc. SPIE-Int. Soc. Opt. Eng.*, 2011, **4259**, 102–109.

11 P. L. Russo, A. J. Wozniak, L. Polin, D. Capps, W. R. Leopold, L. M. Werbel, L. Biernat, M. E. Dan and T. H. Corbett, Antitumor efficacy of PD115934 (NSC 366140) against solid tumors of mice, *Cancer Res.*, 1990, **50**, 4900–4905.

12 Y. Mikata, K. Mogami, M. Kato, I. Okura and S. Yano, Synthesis, characterization, interaction with DNA, and antitumor activity of a *cis*-dichloroplatinum(II) complex linked to an intercalator *via* one methylene chain, *Bioorg. Med. Chem. Lett.*, 1997, **7**, 1083–1086.

13 N. Agorastos, L. Borsig, A. Renard, P. Antoni, G. Viola, B. Spingler, P. Kurz and R. Alberto, Cell-specific and nuclear targeting with $[M(CO)_3]^+$ (M = ^{99m}Tc, Re)-based complexes conjugated to acridine orange and bombesin, *Chem.–Eur. J.*, 2007, **13**, 3842–3852.

14 K. Zelenka, L. Borsig and R. Alberto, Metal complex mediated conjugation of peptides to nucleus targeting acridine orange: a modular concept for dual-modality imaging agents, *Bioconjugate Chem.*, 2011, **22**, 958–967.

15 A. Adams, J. M. Guss, W. A. Denny and L. P. G. Wakelin, Structure of 9-amino-[*N*-(2-dimethylamino)propyl]acridine-4-carboxamide bound to d(CGTACG)(2): a comparison of structures of d(CGTACG)(2) complexed with intercalatorsin the presence of cobalt, *Acta Crystallogr., Sect. D: Biol. Crystallogr.*, 2004, **60**, 823–828.

16 W. M. Cholody, S. Martelli and J. Konopat, Chromophore-modified antineoplastic imidazoacridinones. Synthesis and activity against murine leukemias, *J. Med. Chem.*, 1992, **35**, 378–382.

17 H. B. Zhuang, W. J. Tang, J. Y. Yu and Q. H. Song, Acridin-9-ylmethoxycarbonyl (Amoc): a new photochemically removable protecting group for alcohols, *Chin. J. Chem.*, 2006, **24**, 1465–1468.

18 A. M. Piloto, G. Hungerford, S. P. G. Costa and M. S. T. Gonçalves, Acridinyl methyl esters as photoactive precursors in the release of neurotransmitter amino acids, *Photochem. Photobiol. Sci.*, 2013, **12**, 339–347.

19 Y. Mikata, K. Mogami, M. Kato, I. Okura and S. Yano, Synthesis, characterization, interaction with DNA, and antitumor activity of a *cis*-dichloroplatinum(II) complex linked to an intercalator *via* one methylene chain, *Bioorg. Med. Chem. Lett.*, 1997, **7**, 1083–1086.

20 J. V. Morris, M. A. Mahaney and J. R. Huber, Fluorescence quantum yield determinations. 9,10-Diphenylanthracene as a reference standard in different solvents, *J. Phys. Chem.*, 1976, **80**, 969–974.

21 E. L. Wehry, in *Practical Fluorescence*, ed. G. G. Guilbault, Marcel Dekker, Inc., New York, 1990.

22 L. Goodman and R. W. Harrell, Calculation of n→π* transition energies in *N*-heterocyclic molecules by a one-electron approximation, *J. Chem. Phys.*, 1959, **30**, 1131–1138.

23 E. T. Ryan, T. Xiang, K. P. Johnston and M. A. Fox, Absorption and fluorescence studies of acridine in subcritical and supercritical water, *J. Phys. Chem. A*, 1997, **101**, 1827–1835.

24 (*a*) C. A. Parker, A new sensitive chemical actinometer. I. Some trials with potassium ferrioxalate, *Proc. R. Soc. London, Ser. A*, 1953, **220**, 104–116; (*b*) C. G. Hatchard and C. A. Parker, A new sensitive chemical actinometer. II. Potassium ferrioxalate as a standard chemical actinometer, *Proc. R. Soc. London, Ser. A*, 1956, **235**, 518–536.

25 J. F. Rabek, *Radiometry and actinometry: Experimental methods in photochemistry and photophysics*, Wiley, New York, 1982; vol. 2, p. 944.

26 H. Suzuki and Y. Tanaka, An unusually acidic methyl group directly bound to acridinium cation, *J. Org. Chem.*, 2001, **66**, 2227–2231.

27 T. Mosmann, Rapid colorimetric assay for cellular growth and survival: application to proliferation and cytotoxicity assays, *J. Immunol. Methods*, 1983, **65**, 55–63.

28 M. A. Schumacher, K. M. Piro and W. Xu, Insight into F plasmid DNA segregation revealed by structures of SopB and SopB-DNA complexes, *Nucleic Acids Res.*, 2010, **38**, 4514–4526.

29 A. W. Schüttelkopf and D. M. F. Aalten van, PRODRG: a tool for high-throughput crystallography of protein–ligand complexes, *Acta Crystallogr.*, 2004, **D60**, 1355–1363.

30 B. R. Brooks, C. L. Brooks III, A. D. Mackerell, L. Nilsson, R. J. Petrella, B. Roux, Y. Won, G. Archontis, C. Bartels, S. Boresch, A. Caflisch, L. Caves, Q. Cui, A. R. Dinner, M. Feig, S. Fischer, J. Gao, M. Hodoscek, W. Im, K. Kuczera, T. Lazaridis, J. Ma, V. Ovchinnikov, E. Paci, R. W. Pastor, C. B. Post, J. Z. Pu, M. Schaefer, B. Tidor, R. M. Venable, H. L. Woodcock, X. Wu, W. Yang, D. M. York and M. Karplus:, CHARMM: the biomolecular simulation program, *J. Comp. Chem.*, 2009, **30**, 1545–1614.

31 G. M. Morris, D. S. Goodsell, R. Huey and A. J. Olson, Distributed automated docking of flexible ligands to proteins: parallel applications of AutoDock 2.4, *J. Comput.-Aided Mol. Des.*, 1996, **10**, 293–304.

32 W. L. DeLano, *The PyMOL Molecular Graphics System*; DeLano Scientific, San Carlos, CA, 2004, http://pymol.sourceforge.net/

